Petit et al., http://www.jcb.org/cgi/content/full/jcb.201307084/DC1

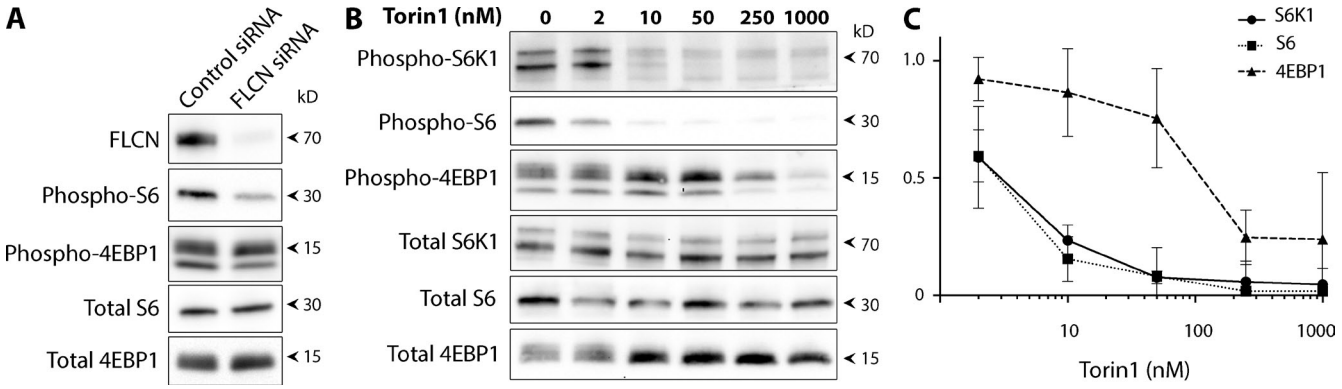

Figure S1. **Characterization of the sensitivity of mTORC1 target phosphorylation to FLCN KD and torin 1 treatment.** (A) Western blot analysis of the phosphorylation of reporters of mTORC1 activity ± FLCN siRNA under basal cell growth conditions (phospho-S6 = S235/236, phospho-4EBP1= T37/T46). (B) Western blot analysis of the phosphorylation of reporters of mTORC1 activity after incubation for 2 h with increasing amounts of Torin1 (mTOR inhibitor). (C) Quantification of the effects of Torin1 on S6K1, S6, and 4EBP1 phosphorylation (mean ± SEM, *n* = 3 experiments). Data obtained from HeLa cells.

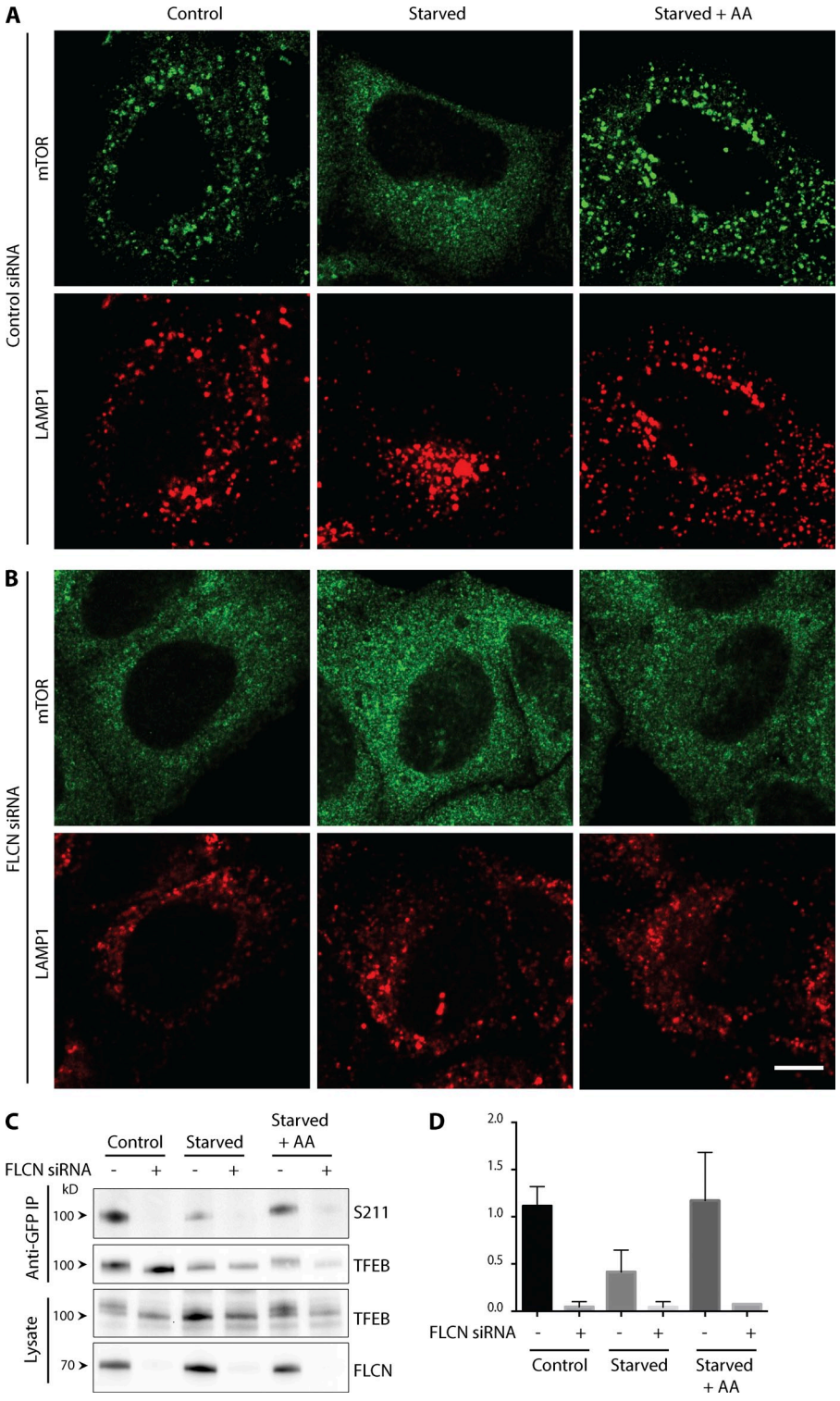

Figure S2. **Investigation of the effects of FLCN KD on the responsiveness of mTOR localization and TFEB phosphorylation to amino acid availability.** (A and B) Immunofluorescence analysis showing the effect of starvation (2 h in serum and amino acid–free RPMI) and amino acid re-feeding (20 min 1×MEM amino acid supplement) on mTOR localization ± FLCN knockdown. (C) Immunoblot analysis and quantification (D) of TFEB-GFP (stable HeLa cell line) immunoprecipitations showing the effect of starvation and amino acid re-feeding on TFEB serine 211 phosphorylation ± FLCN knockdown (n = 3 experiments, mean ± SEM; *, $P < 0.01$ by ANOVA). Data obtained from HeLa cells.

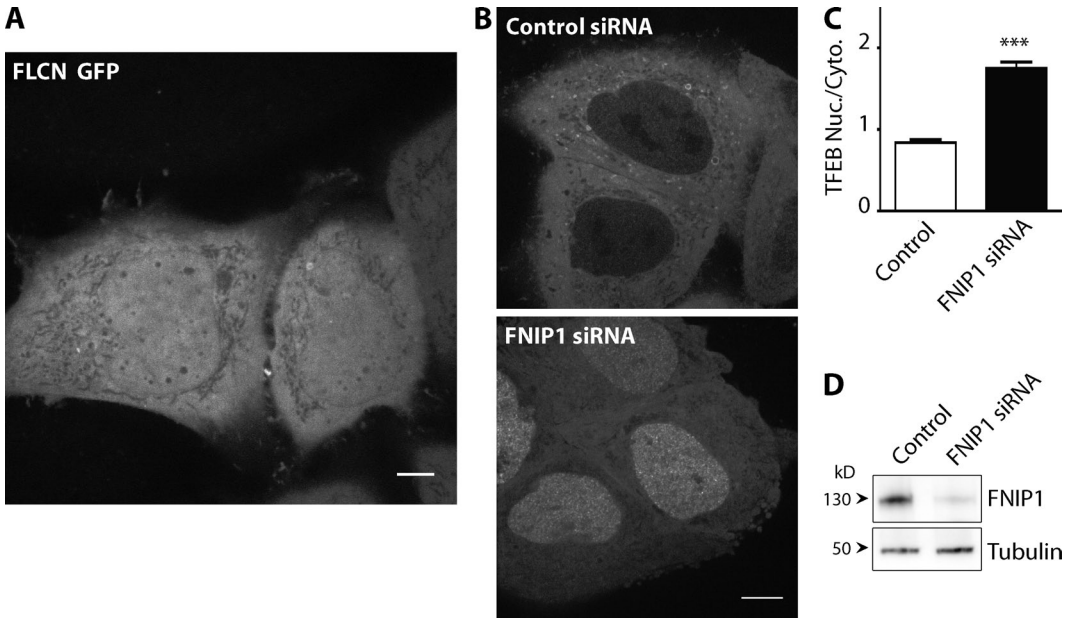

Figure S3. **Role for FNIP1 in the regulation of FLCN and TFEB localization.** (A) Localization of FLCN-GFP. (B) Representative localization of TFEB-GFP ± FNIP1 knockdown. (C) Quantification of the effect of FNIP1 knockdown on the nuclear/cytoplasmic ratio of TFEB-GFP, (n = 3 experiments, mean ± SEM; ***, P < 0.001 by ANOVA with Bonferroni post-test). (D) Western blot analysis showing efficiency of FNIP1 knockdown. All images obtained by live-cell spinning disk confocal microscopy of HeLa cells. Bars = 10 µm. Data obtained from HeLa cells.

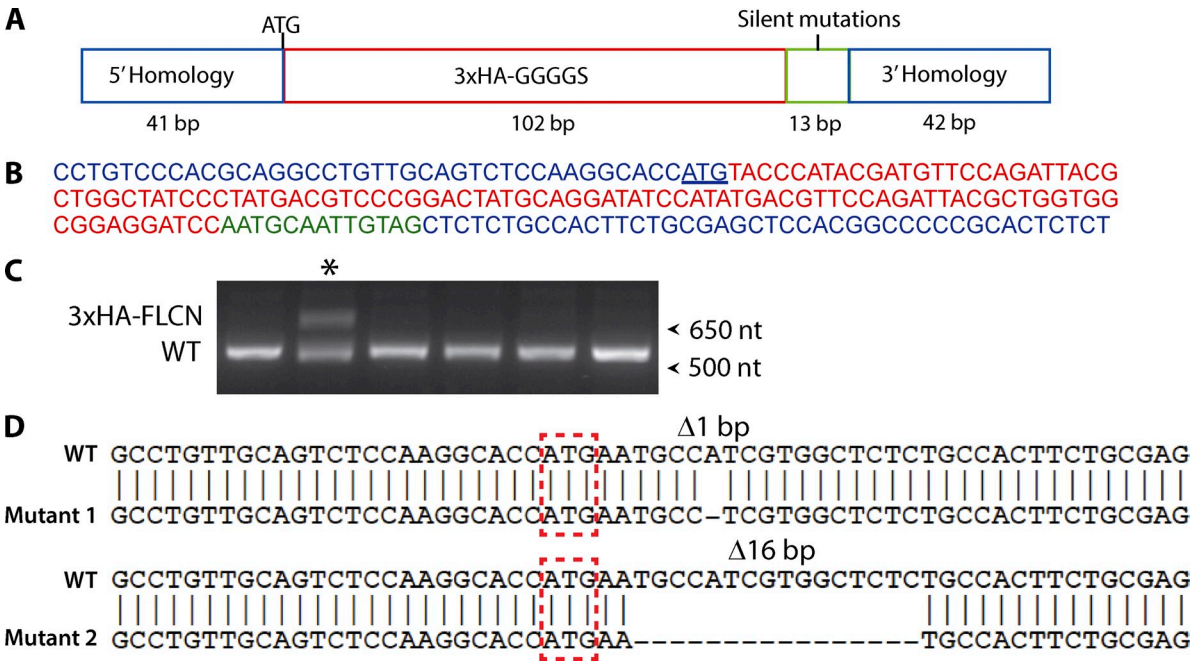

Figure S4. **CRISPR/Cas9 strategy for insertion of 3xHA tag into the endogenous human FLCN genomic locus.** (A) Schematic diagram of the oligonucleotide that was used to direct insertion of the 3xHA encoding sequence into the 5′ end of the human FLCN coding sequence. (B) Sequence of the oligonucleotide outlined in A that uses the same color coding scheme (FLCN start codon is underlined). (C) Screening of clonal cell populations by PCR resulted in the identification of a HeLa cell clone (*) that contained a band (660 bp) corresponding to the insertion of the 3xHA tag into the FLCN locus. The identity of this band was later confirmed by sequencing. (D) Sequence analysis revealed that the lower (~550 bp) bands in the colony identified in C as having the 3xHA insertion (660 bp) contained small deletions of 1 bp and 16 bp, respectively, within the FLCN coding sequence. FLCN start codon is boxed (red dashed line).

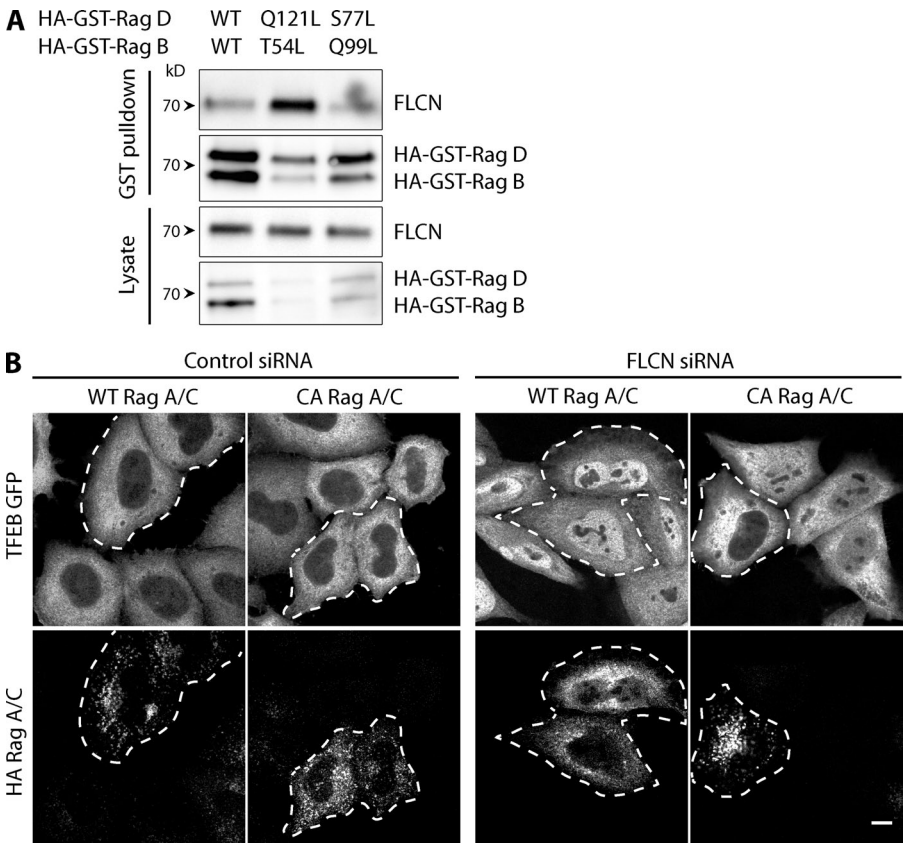

Figure S5. **Relationship between FLCN–Rag interactions and regulation of TFEB subcellular localization.** (A) Immunoblot analysis of GST pull-downs from HEK 293 cells transfected with either HA-GST tagged wild-type RagB+D or the indicated combinations of the constitutively active (RagB Q99L = $RagB^{GTP}$ + RagD S77L = $RagD^{GDP}$) and dominant-negative (RagB T54L = $RagB^{GDP}$ + RagD Q121L = $RagD^{GTP}$) mutants. (B) Immunofluorescence analysis of TFEB-GFP and HA-GST-Rag GTPase localization in control or FLCN KD cells cotransfected with either wild-type Rag A+C or constitutively active (CA) RagA+C (RagA Q66L + RagC S75L) heterodimers (line scanning confocal imaging; bar, 10 µm). Data obtained from HeLa cells.